Journal of Applied Mechanics and Technical Physics, Vol. 51, No. 2, pp. 155–163, 2010

PLANE PROBLEM OF THE IMPACT OF SEVERAL SHOCK PULSES ON A VISCOELASTIC PLATE FLOATING ON A FLUID SURFACE

A. V. Pogorelova

UDC 532.591:539.3:534.1

The impact of a series of sequential and simultaneous pulse loads on the deflection and stress of ice covering a body of water is considered. The effects of the water-body depth, plate thickness, pulse loading conditions, and interpulse interval on the height of the flexural-gravity wave and plate bending stress are analyzed.

Key words: *floating viscoelastic plate, pulse loading, stress–strain state, flexural-gravity wave.*

One method of breaking ice cover is blasting. To increase the destruction area, it is common to use a plurality of spaced apart blasting charges detonated simultaneously or sequentially. In this connection, the problem of using the interference of flexural-gravity waves propagating from different loading sources on ice cover is of great interest [1].

The behavior of ice cover under shock loading has been actively studied during the last few decades (see, for example, works [2, 3] and the bibliography therein). A review of studies of wave formation in ice cover and the behavior of very much large floating structures (VLFSs) on waves is given in [4]. Among the recent papers on the effect of shock pulses on ice cover, we mention [5–9]. Along with pulse load on an infinite plate, studies have been made of flexural-gravity fluctuations of an elastic plate of finite dimensions subjected to periodic loading [10–12].

The present paper considers the deflection of a viscoelastic plate caused by several simultaneous or sequential pulse loads spaced apart from each other.

1. The problem is two-dimensional. Let an infinite viscoelastic ice plate float on the surface of an ideal incompressible fluid. The plate is first in equilibrium, and then, at the times $t_1, t_2, \ldots, t_n$, it is loaded by shock pulses $Y_1, Y_2, \ldots, Y_n$. We consider an odd number of pulses whose points of application are equally spaced a distance l apart. The coordinate origin is attached to the point of application of the pulse Y_i located in the middle of the series of pulses $Y_1, Y_2, \ldots, Y_n$ (in the particular case of a single pulse, the coordinate origin is at the point of application of this pulse), the Ox axis is on the unperturbed plate–fluid interface and the Oz axis is directed upward. The motion of the fluid is considered potential, and its density equal to ρ_2.

According to [13, 14], ice deformation is described by the linear retarded elastic Kelvin–Voigt model.

By analogy with [2], it is assumed that the deflection of the ice plate can be described using the method of superposition of its wave perturbations caused by shock pulses $Y_1, Y_2, \ldots, Y_n$ applied at the points $x_1, x_2, \ldots, x_n$. In this case, the differential equation of small fluctuations of the floating plate is written as

$$\Big(\frac{Gh^3}{3}\Big(1+\tau_{\mathrm{K}}\frac{\partial}{\partial t}\Big)\frac{\partial^4}{\partial x^4}+\rho_1 h\frac{\partial^2}{\partial t^2}+\rho_2 g\Big)w+\rho_2\frac{\partial\Phi}{\partial t}\Big|_{z=0}=-\sum_{r=1}^{n}Y_0\delta(x-x_r)\delta(t-t_r), \tag{1.1}$$

where $G = 0.5E/(1+\nu)$ is the shear elasticity modulus of ice, E is the elasticity modulus of ice in tension and compression, ν is Poisson's ratio for ice, $h(x)$ and $\rho_1(x)$ are the thickness and density of ice, respectively, τ_{K} is the relaxation time of ice stress or the retardation time [13, 14], $w(x,t)$ is the ice plate deflection caused by shock pulses

Institute of Machine Science and Metallurgy, Far East Division, Russian Academy of Sciences, Komsomol'sk-on-Amur 681005; milova@yandex.ru. Translated from Prikladnaya Mekhanika i Tekhnicheskaya Fizika, Vol. 51, No. 2, pp. 16–26, March–April, 2010. Original article submitted October 23, 2008; revision submitted April 10, 2009.

$Y_1, Y_2, \ldots, Y_n$, $\Phi(x,z,t)$ is a function of the fluid velocity potential that satisfies the Laplace equation $\Delta\Phi = 0$, $Y_0\delta(x-x_r)\delta(t-t_r)$ is a function of the shock pulse applied at the point x_r at the time t_r, and $\delta(x)$ and $\delta(t)$ are the Dirac delta-functions, and g is the acceleration due to gravity. Below, the quantities ρ_1 and h are considered constant. In the calculation, as the shear modulus G and density of the plate ρ_1 one should use their normalized values determined as integrated quantities over the plate thickness.

The initial conditions for the function $w(x,t)$ are homogeneous:

$$w(x,0) = \dot{w}(x,0) = 0.$$

The linearized kinematic condition on the ice–water interface is written as

$$\frac{\partial\Phi}{\partial z}\Big|_{z=0} = \frac{\partial w}{\partial t}. \tag{1.2}$$

The boundary condition at the bottom of the water body for the function of the fluid velocity potential $\Phi(x,z,t)$ is given by

$$\frac{\partial\Phi}{\partial z}\Big|_{z=-H} = 0, \tag{1.3}$$

where $H = H_1 - b$, H_1 is the water-body depth and $b = \rho_1 h/\rho_2$ is the ice immersion depth in static equilibrium.

2. In the analytical solution of the problem, it is assumed that the functions $w(x,t)$ and $\Phi(x,z,t)$ satisfy the necessary conditions required to apply a Fourier transform over the variable x:

$$w_{\mathrm{F}}(\gamma,t) = \frac{1}{\sqrt{2\pi}}\int\limits_{-\infty}^{+\infty}\exp\left(-i(\gamma x)\right)w(x,t)\,dx,$$

$$\Phi_{\mathrm{F}}(\gamma,z,t) = \frac{1}{\sqrt{2\pi}}\int\limits_{-\infty}^{+\infty}\exp\left(-i(\gamma x)\right)\Phi(x,z,t)\,dx.$$

Similarly to [7, 8, 13], we apply a Fourier transform to Eq. (1.1) using conditions (1.2) and (1.3) obtain the following second-order equation for the transform w_{F}:

$$\ddot{w}_{\mathrm{F}}m(\gamma) + \dot{w}_{\mathrm{F}}k(\gamma) + w_{\mathrm{F}}c(\gamma) = -\sum_{r=1}^{n}\frac{Y_0\exp\left(-ix_r\gamma\right)}{\sqrt{2\pi}}\,\delta(t-t_r), \tag{2.1}$$

where

$$k(\gamma) = \tau_{\mathrm{K}}\,\frac{Gh^3\gamma^4}{3}, \qquad m(\gamma) = \rho_1 h + \frac{\rho_2}{\gamma\tanh\,(\gamma H)}, \qquad c(\gamma) = \rho_2 g + \frac{Gh^3\gamma^4}{3}.$$

Using a Laplace transform and homogeneous initial conditions, from Eq. (2.1) for the function w_{F} we obtain

$$w_{\mathrm{F}} = \sum_{r=1}^{n} Y_0 w_{r\mathrm{F}}\exp\left(-ix_r\gamma\right),$$

where

$$w_{r\mathrm{F}} = \begin{cases} -\dfrac{1}{\sqrt{cm-k^2/4}}\exp\Big(-\dfrac{k(t-t_r)}{2m}\Big)\sin\Big(\dfrac{t-t_r}{m}\sqrt{cm-\dfrac{k^2}{4}}\Big), & cm-\dfrac{k^2}{4} > 0, \\ -\dfrac{1}{\sqrt{k^2/4-cm}}\exp\Big(-\dfrac{k(t-t_r)}{2m}\Big)\sinh\Big(\dfrac{t-t_r}{m}\sqrt{\dfrac{k^2}{4}-cm}\Big), & \dfrac{k^2}{4}-cm > 0, \\ -\dfrac{t-t_r}{m}\exp\Big(-\dfrac{k(t-t_r)}{2m}\Big), & cm-\dfrac{k^2}{4} = 0. \end{cases}$$

Applying an inverse Fourier transform, we write the sought function $w(x,t)$ in the form

$$w(x,t) = \sum_{r=1}^{n}\frac{1}{\pi}\int\limits_{0}^{\infty} Y_0 w_{r\mathrm{F}}\cos\left(\gamma(x-x_r)\right)d\gamma. \tag{2.2}$$

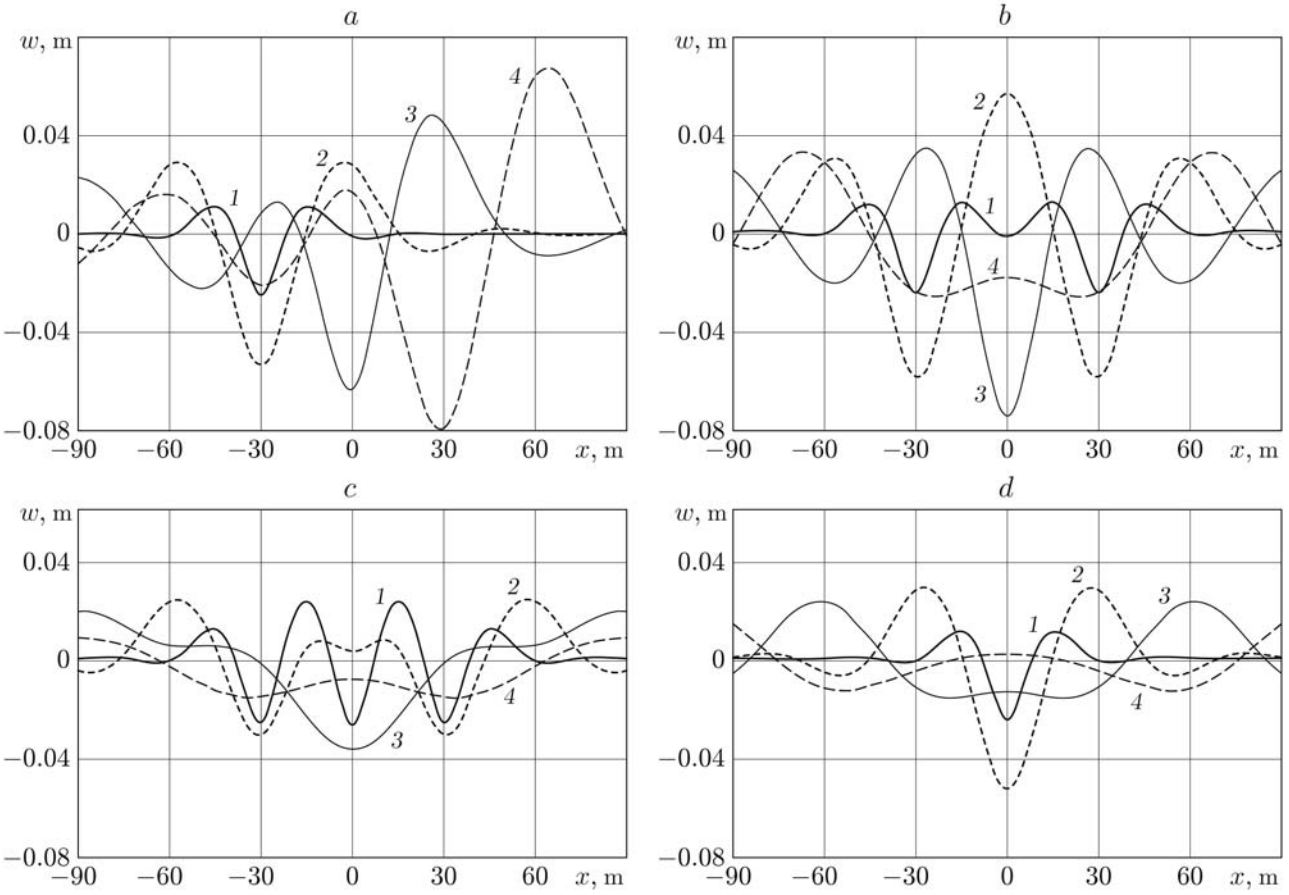

Fig. 1. Deflection of the ice plate versus coordinate x for $H = 5$ m and $h = 0.5$ m in various loading modes: (a–c) loading by three pulses: (a) sequential mode ($x_1 = -30$ m and $t_1 = 0$; $x_2 = 0$ and $t_2 = 4.29$ sec; $x_3 = 30$ m and $t_3 = 8.58$ sec); (b) sequential-opposed mode ($x_1 = -30$ m and $t_1 = 0$; $x_2 = 0$ and $t_2 = 4.29$ sec; $x_3 = 30$ m and $t_3 = 0$); (c) simultaneous mode ($x_1 = -30$ m, $x_2 = 0$, and $x_3 = 30$ m; $t_1 = t_2 = t_3 = 0$); (d) loading by a single pulse ($x_1 = 0$ and $t_1 = 0$) for $t = 0.1$ sec (1), 1 (2), 5 (3), and 10 (4).

The bending stress is calculated from the formula

$$\sigma(x,t) = -2Gh\Big(\frac{\partial^2 w(x,t)}{\partial x^2} + \tau_{\mathrm{K}}\,\frac{\partial^3 w(x,t)}{\partial t\,\partial x^2}\Big). \tag{2.3}$$

3. Calculations using formulas (2.2) and (2.3) were performed for the following parameters of the ice plate and water body: $\rho_2 = 1000$ kg/m^3, $\rho_1 = 900$ kg/m^3, $\nu = 1/3$, $E = 5 \cdot 10^9$ N/m^2, $h = 0.5$–2.5 m, $H = 1$–500 m, $\tau_{\mathrm{K}} = 0.69$ sec, and $Y_0 = 5 \cdot 10^4$ N/m^2. The relaxation time τ_{K} was chosen in accordance with experimental data [15].

The following modes of loading by pulses $Y_1, Y_2, \ldots, Y_n$ are considered:

— sequential mode (the pulses are triggered in the sequence of their arrangement $Y_1, Y_2, \ldots, Y_n$);

— sequential-opposed mode (at the initial time, the pulses located at the edges of the series Y_1 and Y_n are triggered, then the pulses Y_2 and Y_{n-1}, and so on; the pulse in the middle of the series of pulses is the last to be triggered);

— simultaneous mode (at the initial time, all pulses $Y_1, Y_2, \ldots, Y_n$) are triggered at the initial time;

— single (one pulse is triggered at the initial time).

In the sequential and sequential-opposed modes, the time interval between the pulses is calculated by the formula

$$T = l/u, \tag{3.1}$$

where u is the presumed propagation velocity of the largest deflection of the flexural-gravity wave in the ice cover.

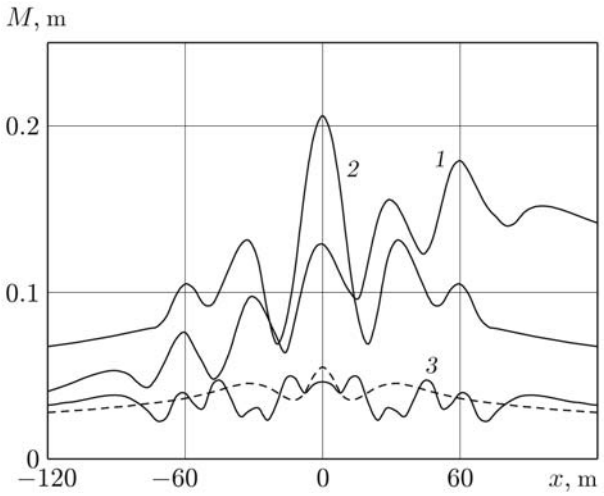

Fig. 2. Height of the flexural-gravity wave versus coordinate x for $H = 5$ m and $h = 0.5$ m in different loading modes: (1–3) loading by five pulses: 1) sequential mode ($t_1 = 0$, $t_2 = 4.29$ sec, $t_3 = 8.57$ sec, $t_4 = 12.86$ sec, and $t_5 = 17.14$ sec); 2) sequential-opposed mode ($t_1 = t_5 = 0$, $t_2 = t_4 = 4.29$ sec, and $t_3 = 8.57$ sec); 3) simultaneous mode ($t_1 = t_2 = t_3 = t_4 = t_5 = 0$); dashed curve corresponds to loading by a single pulse ($x_1 = 0$ and $t_1 = 0$).

Figure 1 shows deflections of the ice plate in the different modes of loading by three pulses for a water-body depth $H = 5$ m and ice-cover thickness $h = 0.5$ m. Under the assumption that the velocity of the flexural-gravity wave under shallow-water conditions is approximately equal to $u = \sqrt{gH}$ [3, 13], the time interval between shock pulses in the sequential and sequential-opposed modes is calculated by formula (3.1).

An analysis of Fig. 1 shows that, in the sequential and sequential-opposed loading modes, the ice plate deflections are larger than those in the simultaneous mode. This is due to the fact that, in the sequential and sequential-opposed modes (see Fig. 1a and b), each subsequent pulse is applied to a specified point of the plate at approximately the time when the base of the largest deflection of the flexural-gravity wave reaches this point. Thus, each subsequent pulse leads to an increase in the amplitude of the ice-plate deflection. This is supported by modeling experiments [1]. An analysis of the behavior of ice-plate deflection in the simultaneous loading mode (see Fig. 1c) shows that, with time, the flexural-gravity waves propagating from each source of pulses damp each other, with the absolute value of the deflection being comparable to the deflection value in the case of loading by a single pulse (see Fig. 1d).

It is obvious that, with time t, the plate deflection $w(x, t)$ at any point x reaches the maximum and minimum values. The difference between the maximum and minimum deflections $w(x, t)$ at the specified point x will be called the height of the flexural-gravity wave at the point x and will be denoted by $M(x)$.

Figure 2 shows curves of $M(x)$ for $H = 5$ m and $h = 0.5$ m for the sequential, sequential-opposed, and simultaneous modes of operation of five impactors located at the points $x_1 = -60$ m, $x_2 = -30$ m, $x_3 = 0$, $x_4 = 30$ m, and $x_5 = 60$ m. For comparison, the figure shows the height of the flexural-gravity wave in the case of a single pulse applied at the point $t_1 = 0$ at the time $x_1 = 0$ (dashed curve in Fig. 2). The time interval between the operation of shock pulses for the cases of sequential and sequential-opposed loading calculated by formula (3.1) for $u = \sqrt{gH}$.

In Fig. 2, it is evident that, compared to the simultaneous mode of triggering of shock pulses, the sequential and sequential-opposed modes lead to a more than a factor of four increase in the height of the flexural-gravity wave $M(x)$. The height of the wave $M(x)$ reaches the maximum values at the points of application of the last pulses in the sequential ($x = 60$ m) and sequential-opposed modes ($x = 0$). In this case, the quantity $M(0)$ for the sequential-opposed mode is larger than the quantity $M(60)$ for the sequential mode. In the case of simultaneous triggering of five pulses, the maximum wave height is comparable to the height of waves in the case of loading by a single pulse, and the effect of the pulse covers a wider area.

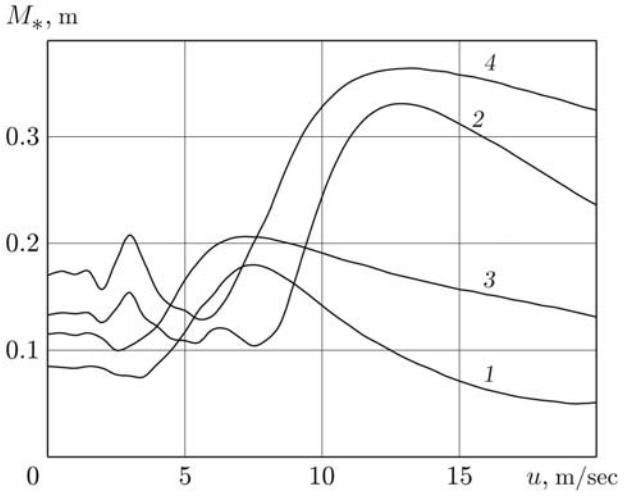

Fig. 3

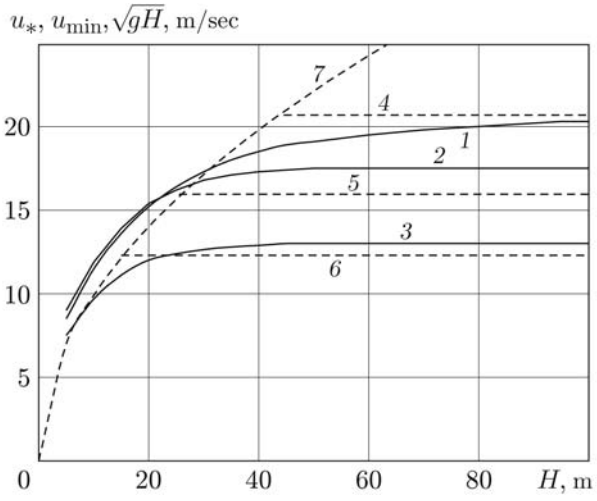

Fig. 4

Fig. 3. Maximum height of the flexural-gravity wave M_* versus velocity u in the sequential (1 and 2) and sequential-opposed (3 and 4) loading modes for $h = 0.5$ m and $H = 5$ (1 and 3) and 100 m (2 and 4).

Fig. 4. Velocities versus water-body depth H for $h = 2$ (1 and 4), 1 (2 and 5), 0.5 m (3 and 6); curves 1–3 refer to u_*, curves 4–6 refer to $u = u_{\min}$ and curve 7 refers to $u = \sqrt{gH}$.

Let us analyze the effect of the velocity u in the formula for the time interval (3.1) on the maximum wave height M_* for the case of loading by five pulses separated by a distance $l = 30$ m ($x_1 = -60$ m, $x_2 = -30$ m, $x_3 = 0$, $x_4 = 30$ m, and $x_5 = 60$).

Figure 3 gives values of the wave height $M_* = M(60)$ at $h = 0.5$ m for the sequential loading mode (curves 1 and 2) and $M_* = M(0)$ for the sequential-opposed mode (curves 3 and 4). It is obvious that, for any values of the velocity u in the sequential-opposed mode, the wave height is greater than that in the sequential mode. This is supported by model experiments [1]. By choosing the velocity u, it is possible to considerably increase the largest height of the flexural-gravity wave in the case of deep water compared to the case of shallow water. We note that curves 1 and 2 (sequential mode) have more distinct maxima than curves 3 and 4 (sequential-opposed mode). In the case $h = 0.5$ m, these maximum values occur at $u \approx \sqrt{gH}$ for shallow water and at $u \approx u_{\min}$ for deep water [$u_{\min} = 2(Dg^3/(27\rho_2))^{1/8}$ is the minimum phase velocity of flexural-gravity waves of ice cover for a water body of great depth [3, 13]; $D = Eh^3/(12(1-\nu^2))$ is the cylindrical rigidity of the plate (at $h = 0.5$ m and $E = 5 \cdot 10^9$ N/m^2 $u_{\min} \approx 12.3$ m/sec)].

We denote by u_* the propagation velocity u of the largest deflection of the flexural-gravity wave corresponding to the largest value of M_* in the sequential mode. It is obvious that the quantity u_* should depend on the parameters of the ice plate and water body.

Figure 4 shows curves of the velocities u_*, $u = u_{\min}$, and $u = \sqrt{gH}$ versus water-body depth H for various thicknesses of ice cover h. It is evident that, in the case of shallow water, the wave height reaches the maximum when u is 10–20% larger than the value $u = \sqrt{gH}$ (this is supported by model experiments [1]), and in the case of deep water, when $u \approx u_{\min}$. Thus, to increase the height of the flexural-gravity wave using sequential (or sequential-opposed) pulse loading mode, it is necessary to calculate the time interval T between pulses using the propagation velocity of this wave $u \approx (1.1\text{–}1.2)\sqrt{gH}$ for shallow water and $u = u_{\min}$ for deep water. We note that the curves of $u_*(H)$ in Fig. 4 correspond to the critical velocities of motion of a const loading on ice cover [3, 13].

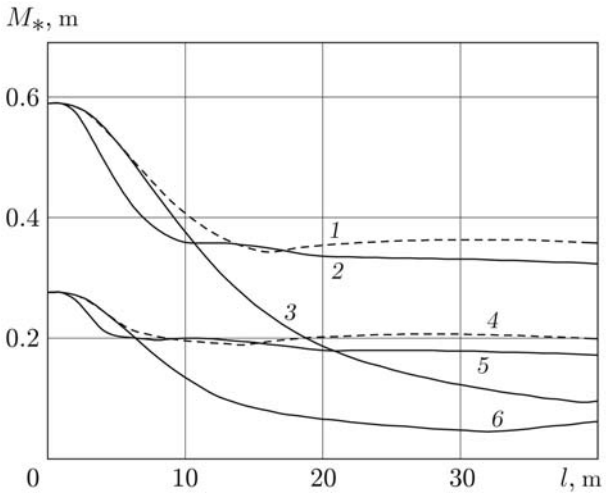

Fig. 5. Maximum wave height M_* versus distance between the points of application of pulses l at $h = 0.5$ m and various modes of operation of five pulses: sequential-opposed mode (1 and 4), sequential mode (2 and 5), simultaneous mode (3 and 6); curves 1–3 refer to $u = u_{\min}$ and $H = 100$ m; curves 4–6 refer to $u = \sqrt{gH}$ and $H = 5$ m.

Figure 5 gives curves of the maximum wave height M_* versus distance between the points of application of pulses l for $h = 0.5$ m and various modes of operation of five pulses for $u = u_{\min}$, $H = 100$ m (curves 1–3), and $u = \sqrt{gH}$, $H = 5$ m (curves 4–6). The maximum values of the wave height M_* in the sequential (curves 2 and 5) and sequential-opposed modes (curves 1 and 4) are calculated at the points of application of the last pulses, and in the simultaneous mode (curves 3 and 6), at the point of application of the pulse located in the middle of the series of pulses. As follows from Fig. 2, it is difficult to distinguish a point x at which the wave height takes the largest value in the simultaneous mode; therefore, for the results presented in Fig. 5, in the simultaneous mode, we used the value of wave height at one of the local maximum points, namely, at the point of application of the pulse located in the middle of the series of pulses.

An analysis of Fig. 5 shows that the flexural-gravity wave in an ice plate of thickness $h = 0.5$ m reaches the largest height if the distance between the points of application of pulses $l \leqslant 1$ m. In this case, the choice of the mode does not influence the maximum ice-plate deflection. In the case of small distances between pulses (for $h = 0.5$ m, 1 m $< l <$ 3 m for shallow water and 1 m $< l <$ 5 m for deep water), the wave height for the simultaneous and sequential-opposed modes is the same and exceeds the wave height in the sequential mode. As the distance between the pulses increases, the sequential mode becomes comparable to the sequential-opposed mode while the simultaneous mode is less effective, at least, in the case where the distance between the points of application of the pulses l is not equal to the wave length.

In Fig. 5, it is evident that the wave height in the sequential-opposed loading mode is greater than that in the simultaneous mode for all l, except in the range of small distances l in which the wave height in the specified modes is identical. We choose a value l_* such that, for $l \geqslant l_*$, the maximum height of the flexural-gravity wave M_* in the sequential-opposed mode exceeds that in the simultaneous mode by more than 5%. Figure 6 gives the distance l_* versus ice-cover thickness h for various water-body depths. It is evident that for the set of all values of h and l in the region above curves 1–5 in Fig. 6, the height of the flexural-gravity wave in the sequential-opposed mode is greater than that in the simultaneous mode. In the region below curves 1–5, the maximum wave height in the specified modes is approximately identical. We call this region the range of applicability of the simultaneous mode. From Fig. 6, it follows that if the water-body depth H is great, this region broadens with increasing ice-cover thickness h. In the case of small depths of the water body H for any ice-cover thickness h, the range of applicability of the simultaneous mode is bounded by small distances l between the points of application of the pulses.

Let us consider the behavior of the bending stress $\sigma(x, t)$ at the points corresponding to the maximum wave height M_*. From formulas (2.2) and (2.3), it follows that $\sigma(x, t) \overset{t \to t_r}{\longrightarrow} \infty$ for $\tau_{\mathrm{K}} \neq 0$. However, numerical calculations

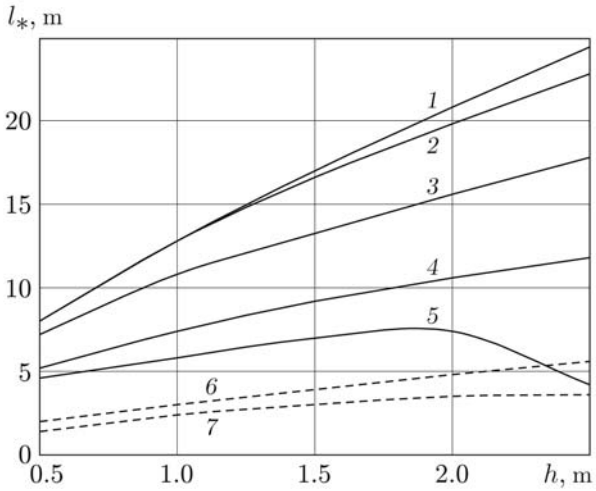

Fig. 6. Critical distance between the points of application of pulses l_* versus ice-cover thickness h for various water-body depths: $H = 500$ m (1), 100 (2 and 6), 25 (3), 5 (4 and 7), and 1 m (5); dashed curves correspond to the minimum values l_* for which the largest value of $S(x)$ for the sequential-opposed mode of loading by five pulses exceeds the largest value of $S(x)$ for the simultaneous mode by more than 5%.

show that the improper integral $\int_0^\infty \sigma(x,t)\,dt$ is a convergent one for any finite number of pulses applied to the plate. Therefore, to analyze the effect of several pulses on the bending stress, we introduce an integrated index of plate stresses

$$S(x) = \int_0^\infty |\sigma(x,t)|\,dt.$$

It is calculated by summing all bending stresses in the plate due to the impact of several pulses and then by calculating the improper integral of the absolute value of the obtained quantity.

Figure 7 gives curves of $S(x)$ for three pulses applied to the plate at the points $x_1 = -30$ m, $x_2 = 0$, and $x_3 = 30$ m for a water-body depth $H = 5$ m and ice-cover thickness $h = 0.5$ m. The time interval between the sequential impact of the pulses calculated by formula (3.1) for $u = \sqrt{gH}$. It is evident that, in the sequential and sequential-opposed loading modes, the stresses in the plate are two times larger than those in the case of simultaneous application of pulses. At the points of application of the pulses corresponding to the maximum values of the wave height M_*, the integrated stress index $S(x)$ also takes the maximum values.

An analysis of the effects of the water-body depth, ice-cover thickness, and mode of application of pulses on the dependence $S(x)$ shows that the integrated bending-stress index $S(x)$ and the wave height reach the maximum values in the sequential-opposed loading mode. In this case, the range of the parameter l in which the quantity $S(x)$ takes the same large values in the simultaneous loading mode as in the sequential-opposed mode is confined to small distances between the points of application of pulses. This is confirmed by Fig. 6, which shows the minimum values l_* for which the largest value of $S(x)$ in the sequential-opposed mode of application of five pulses is more than 5% larger than that in the simultaneous mode (curves 6 and 7 for $H = 100$, 5 m, respectively).

Figure 8 shows curves of the maximum wave height M_* and integrated parameter S_* versus water-body depth H in the sequential-opposed mode of operation of five pulses equally separated by a distance $l = 30$ m. It is evident that an increase in the water-body depth from the value $H = 5$ m to $H = 100$ m leads to an significant (almost twice) increase in the wave height but has little effect on the bending stress in the ice plate.

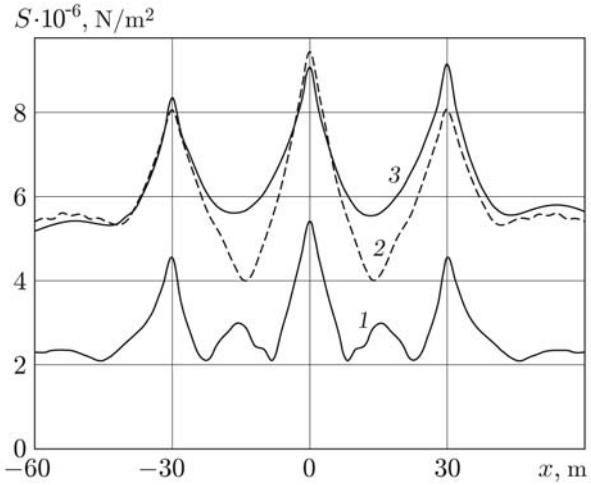

Fig. 7. Integrated stress index S versus coordinate x in the plate at $H = 5$ m and $h = 0.5$ m in various loading modes by three pulses located at the points $x_1 = -30$ m, $x_2 = 0$, $x_3 = 30$ m: 1) simultaneous mode ($t_1 = t_2 = t_3 = 0$); 2) sequential-opposed mode ($t_1 = t_3 = 0$ and $t_2 = 4.29$ sec); 3) sequential mode ($t_1 = 0$, $t_2 = 4.29$ sec, and $t_3 = 8.57$ sec).

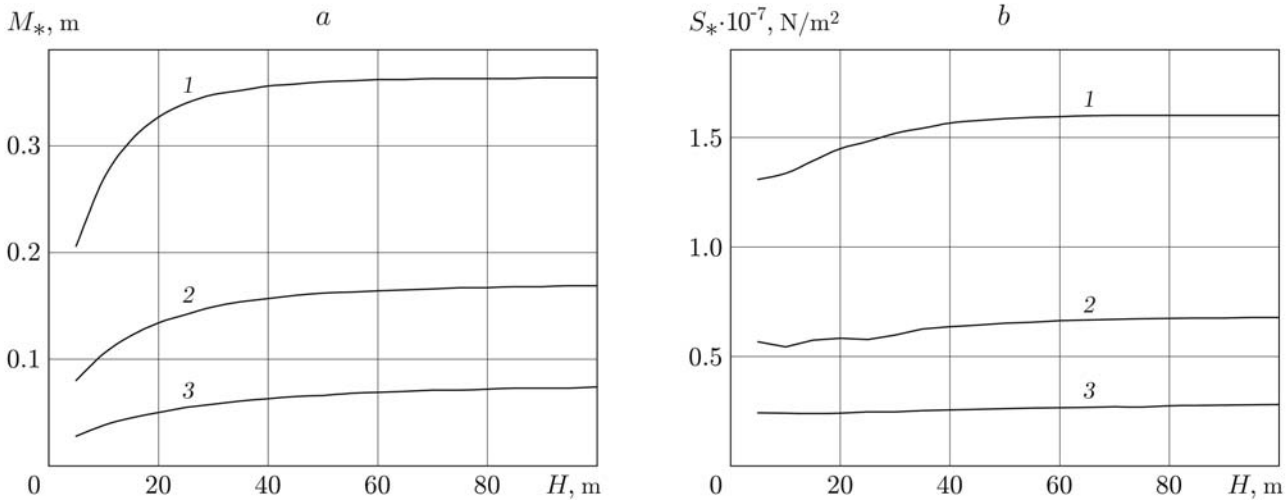

Fig. 8. Maximum wave height M_* (a) and maximum bending stresses in the plate (b) versus water-body depth H for ice-cover thicknesses $h = 0.5$ (1), 1 (2), and 2 m (3).

We note that an increase in the power of the single pulse leads to an increase in the bending stress at the point of application of the load. Furthermore, in the vicinity of this point, the bending stress can exceed the bending strength of ice and cause destruction of the plate, but the area of destruction will be insignificant.

4. The results obtained support the assumptions [1] that, in the sequential and sequential-opposed modes of pulse loading, the amplitude of ice-plate deflection and bending stresses can be increased compared to the simultaneous mode of pulse loading. This, however is possible only if the distance between the points of application of pulses is larger than a certain value l_*, which depends on the water-body depth and ice-cover thickness. If the distance between the points of application of pulses is smaller than l_*, the wave height and the bending stress in the simultaneous mode take the same values as in the sequential-opposed mode.

The wave height and the bending stress reach the maximum values at the points of application of pulses, and in the sequential and sequential-opposed modes, the largest are reached at the points of application of the last pulses.

For optimization of the sequential and sequential-opposed modes, the time intervals between pulses should be calculated from formula (3.1) for velocity $u \approx (1.1\text{–}1.2)\sqrt{gH}$ for shallow water or $u \approx u_{\min}$ for deep water. The wave height and bending stress in the sequential-opposed loading mode are larger than those in the sequential mode.

Although increasing the water-body depth leads to an increase in the height of the flexural-gravity wave at the points of application of pulses, but it does not introduce significant changes to the bending stress in the ice plate.

REFERENCES

1. V. M. Kozin, *Resonant Method of Ice Cover Destruction. Inventions and Experiments* [in Russian], Akad. Estestvoznaniya, Moscow (2007).
2. A. D. Kerr, "The bearing capacity of floating ice plates subjected to static or quasi-static loads," *J. Glaciology*, **17**, No. 76, 229–268 (1976).
3. V. A. Squire, R. J. Hosking, A. D. Kerr, and P. J. Langhorne, *Moving Loads on Ice Plates*, Kluwer, Dordrecht (1996).
4. V. A. Squire, "Synergies between VLFS hydroelasticity and sea ice research," *Int. J. Offshore Polar Eng.*, **18**, No. 4, 241–253 (2008).
5. D. Q. Lu and S. Q. Dai, "Generation of transient waves by impulsive disturbances in an inviscid fluid with ice-cover," *Arch. Appl. Mech.*, **76**, 49–63 (2006).
6. D. Q. Lu and S. Q. Dai, "Flexural-and capillary-gravity waves due to fundamental singularities in an inviscid fluid of finite depth," *Int. J. Eng. Sci.*, **46**, No. 3, 1183–1193 (2008).
7. V. M. Kozin and A. V. Pogorelova, "Mathematical modeling of shock loading of a solid ice cover," *Int. J. Offshore Polar Eng.*, **16**, No. 1, 1–4 (2006).
8. L. A. Tkacheva, "Motion of a system of seismic sources over ice on a water body under the action of a pulse," *J. Appl. Mech. Tech. Phys.*, **48**, No. 2, 271–278 (2007).
9. V. D. Zhestkaya and V. M. Kozin, "Numerical solution of the problem of the effect of a shock pulse on an ice sheet," *J. Appl. Mech. Tech. Phys.*, **49**, No. 2. 285–290 (2008).
10. L. A. Tkacheva, "Impact of a periodic load on a floating elastic plate," *Izv. Ross. Akad. Nauk, Mekh. Zhidk. Gaza*, No. 2, 132–146 (2005).
11. I. V. Sturova and A. A. Korobkin, "Two-dimensional problem of periodic loading on the surface of an elastic plate floating on the surface of an infinitely deep fluid," *J. Appl. Mech. Tech. Phys.*, **46**, No. 3, 355–364 (2005).
12. A. A. Korobkin and T. I. Khabakhpasheva, "Construction of exact solutions in the problem of a floating plate," *Prikl. Mat. Mekh.*, **71**, No. 2. 321–328 (2007).
13. D. E. Kheisin, *Ice Cover Dynamics* [in Russian], Gidrometeoizdat, Leningrad (1967).
14. A. M. Freudenthal and H. Geiringer, *The Mathematical Theories of the Inelastic Continuum*, Springer, Berlin (1958).
15. T. Takizava, "Deflection of a floating sea ice sheet induced by a moving load," *Cold Reg. Sci. Technol.*, **11**, 171–180 (1985).